International Journal of Modern Physics D
Vol. 16, No. 12A (2007) 2245–2258

A LABORATORY TEST OF THE EQUIVALENCE PRINCIPLE AS PROLOG TO A SPACEBORNE EXPERIMENT

ROBERT D. REASENBERG* and JAMES D. PHILLIPS†

Smithsonian Astrophysical Observatory,
Harvard–Smithsonian Center for Astrophysics,
Cambridge, MA, USA
**reasenberg@cfa.harvard.edu*
†jphillips@cfa.harvard.edu

Received 24 August 2006
Revised 12 September 2006
Communicated by S. G. Turyshev

To test the equivalence principle (EP) to an accuracy of at least $\sigma(\Delta g)/g = 5 \times 10^{-14}$, we are developing a modern Galilean experiment. In our principle-of-equivalence measurement (POEM), we directly examine the relative motion of two test mass assemblies (TMA) that are freely falling. Such an experiment tests both for a possible violation of the weak equivalence principle (WEP) and for new forces that might mimic a WEP violation. For the terrestrial version of the experiment, there are three key technologies. A laser gauge measures the separation of the TMA to picometer accuracy in a second as they fall freely in a comoving vacuum chamber. The motion system launches the TMA from their kinematic mounts inside the chamber and keeps the chamber on a trajectory that mimics free fall until the chamber nears the bottom of its motion. It then "bounces" the chamber back to upward motion in preparation for a new launch of the TMA. A capacitance gauge system measures an additional four degrees of freedom of the motion of each TMA. The resulting estimate of the rotation around and translation along the horizontal axes is used to correct systematic errors. We describe the status of POEM and discuss recent progress.

Keywords: WEP; general relativity.

1. Introduction

One needs look no further than these proceedings to find reasons for more stringent testing of the weak equivalence principle (WEP). The WEP is central to the present accepted theory of gravity, and some theorists argue it is the aspect of general relativity that would most easily manifest a breakdown. The evidence that leads to postulating dark energy may be telling us that we need a new gravity theory. Attempts to create a quantum theory of gravity show a failure of the equivalence principle. Finally, the least well tested of the fundamental forces is gravity, which governs the large-scale structure of the Universe. An experiment that tests for a possible violation of the WEP is also sensitive to new forces.

To test the WEP to an accuracy of at least $\sigma(\Delta g)/g = 5 \cdot 10^{-14}$, we are developing a Galilean principle-of-equivalence measurement (POEM) in which we directly examine the relative motion of a pair of test masses that are freely falling. The test mass assemblies (TMA) will be in free fall in a comoving vacuum chamber for about 0.8 s per "toss," i.e. motion both up and down along a vertical path of about 90 cm. These brief periods of free fall repeat at intervals of a little over a second.

Figure 1 shows the principal components of the first generation measurement system. Inside the vacuum chamber is a single pair of TMA resting on shelves separated by 0.5 m. Each TMA contains a sample of a test substance (A or B) and a corner-cube retroreflector. Conditioned laser light entering at the lower right reaches the beamsplitter, illuminating the optical cavity formed by the two retroreflectors, and is then passed to the detector (upper left). The compensator plate makes possible the alignment of the cavity in the presence of imperfect retroreflectors and a wedged beamsplitter. The vacuum chamber is attached to a cart that rides on a vertical track. The position of the cart is driven by a linear motor inside the track and position feedback is provided by a linear incremental encoder with 20 micron markings. The position loop is closed by a DSP-based controller and PWM amplifier, operating together at 20 kHz.

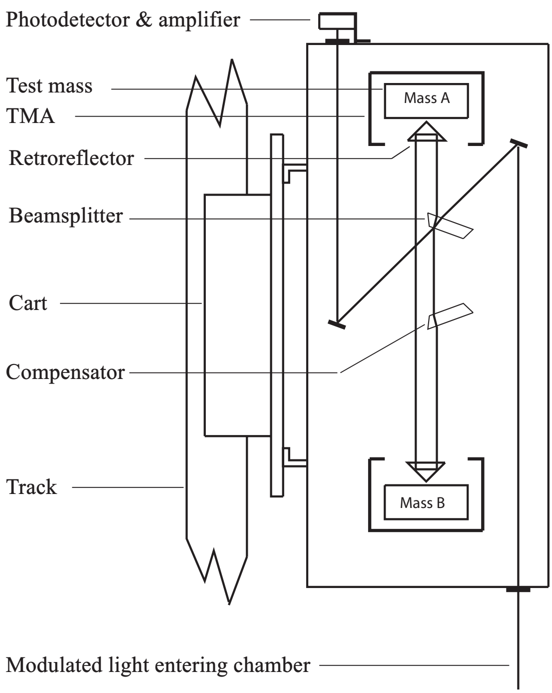

Fig. 1. Principal components of the measurement system.

We are developing POEM in three stages (Gen-I, Gen-II, Gen-III), with possible further development to be defined after the measurement system is working. The measurement system is being designed both for the control of systematic error and, where applicable, to be easily transformed to be space-based. There are three key technologies for POEM: the laser gauge, the capacitance gauge, and the motion system. These will be discussed after a brief description of POEM.

2. POEM

Figure 2 shows the "probe," which comprises all of the components inside the chamber, the chamber's top flange, and the detector for the laser gauge (mounted on top of the flange). One can see the TMA sitting on the shelves as well as the other components of the interferometer. Each TMA appears as a cylinder of 44.5 mm diameter and 36.5 mm height, exclusive of the ball-end tungsten rods that stick out each end and engage the TMA kinematic support. Figure 3 shows an exploded view of a TMA. The retroreflector sits on raised pads in the base plate and is held in place by a flexible ring that has three grooved feet to sit on the retroreflector directly above the raised pads. The ring is loaded by screws from above. The small

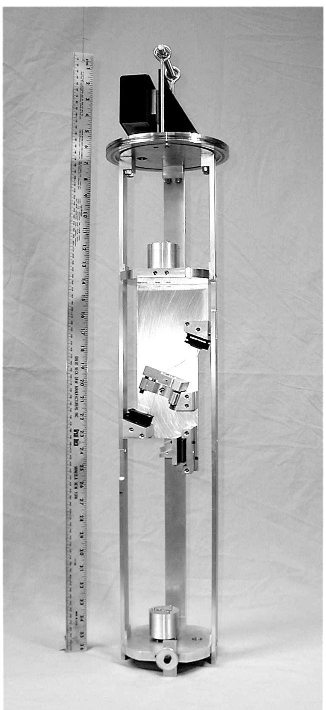

Fig. 2. POEM probe. Some support elements have been removed to make the optics and optical mounts visible. The scale is 36″ long and has both centimeter and inch markings.

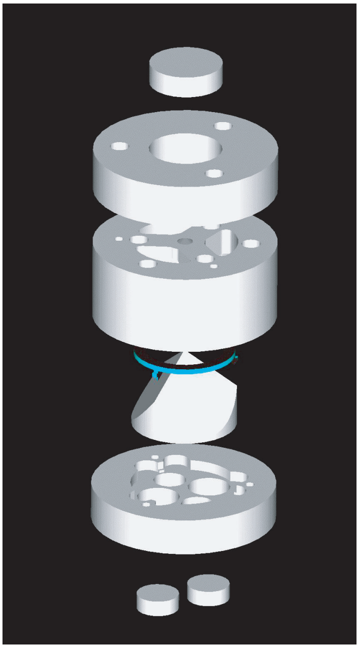

Fig. 3. Exploded view of a TMA.

cylinder at the top is a screw for adjusting the location of the center of mass along the cylindrical axis.

The moving vacuum chamber offers three advantages over the more usual fixed chamber. First, there is no need for mechanisms inside the chamber to drive the motion of the TMA and the TMA-observing devices during each toss. Thus, the vacuum chamber contains no motors, precision bearings, or wall-penetrating shafts that drive high speed motion to sub-mm accuracy. Second, there is no need for a slide (cart plus rails) inside the chamber to guide the motion of the TMA and the TMA-observing devices. The slide would need to provide smooth motion with transverse noise of under about 10 nm. A slide based on ball bearings will not suffice. An air slide, a precision teflon lubricated steel on steel slide, or other low-vibration slide would need to operate in the chamber. The parts that would need to move include most of the probe below the vacuum flange and the cart — about a third of the weight of the present moving assembly. In order to control vibration, the rail inside the chamber would need to be about a third as stiff as the one outside the chamber, and so would be of nearly the same size. Third, the moving chamber can be relatively small and easily opened. A nonmoving chamber would be large and would have to be lifted off with an overhead hoist and therefore be located in a high-bay area. Notwithstanding these advantages, the moving-vacuum-chamber approach has drawbacks. It entails moving tens of kilograms at speeds approaching 5 m/s, which implies large forces and the potential for significant amounts of vibrational energy from which the measurement must be protected. Further, the pump for sustaining (but not for creating) the vacuum must ride with the chamber, although this pump can be of relatively low mass.

The chamber motion repeats in about 1.3 s. The chamber is sent upward at 5 m/s. During the upper portion of the motion, the linear motor and its control system serve to enforce a free-fall trajectory, overcoming friction. At the bottom of the free-fall portion of the motion, the chamber encounters a "bouncer" that passively applies an upward force, absorbs the energy of the falling chamber, and returns the chamber to upward motion in about 0.4 s with a minimum of force required from the motor. The bouncer will be discussed in Sec. 3.1.

In the Gen-II version of POEM, there will be a larger probe (and vacuum chamber) to hold two pairs of TMA (Fig. 4) with a lateral separation of 7 cm. This will permit a double difference observable that cancels many systematic errors. Prominent among these is the gravity gradient, including the vertical component, $dg/dz = 3 \cdot 10^{-7}\,\mathrm{g/m}$. Additionally, there are small components that are time-dependent, including those due to ground-water variation and parked cars on the nearby street.

The Gen-II dual-measurement probe will be modified for Gen-III. With a Gen-III science goal of $\sigma(\Delta g)/g = 5 \cdot 10^{-14}$ and a TMA mass that is 30% test substance, we require a measurement accuracy of $\sigma(\Delta g)/g = 1.5 \cdot 10^{-14}$ for the TMA. This requirement, when combined with the vertical gravity gradient, implies a requirement for absolute distance measurement with an uncertainty under $0.05\,\mu$m. The required laser gauge will be discussed in the next section.

The science goal of $\sigma(\Delta g)/g = 5 \cdot 10^{-14}$ requires careful attention to systematic error. In the Gen-III version of POEM, systematic error is mitigated by a series of interchanges: (1) left–right robotic interchange of TMA on a time scale of perhaps 10 minutes, (2) top–bottom interchange of TMA between runs, and (3) manual interchange of test substance halfway through the experiment if we find that it is needed. These interchanges substantially reduce the biasing due to the gravity gradient and several small effects.

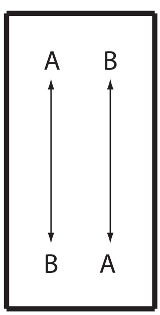

Fig. 4. Locations of the test substances (A and B) inside the TMA in Gen-II and Gen-III. The acceleration difference (left–right) adds any WEP-violating signal and cancels biasing effects.

Some of the error sources depend on parameters that we estimate principally from calibration maneuvers, which we introduce to reduce the impact on measurement time of obtaining these estimates. These error sources include beam alignment and rotation of the TMA in the presence of an offset between the center of mass and the optical reference point (ORP).[a]

We enrich the data set by exaggerating the normally small displacements during calibration maneuvers distributed throughout a run:

(i) At its launch point below the chamber, the laser beam is tipped and tilted forward, back, left, and right of its nominal (vertical) direction.
(ii) Each TMA is pushed (again in four directions) by applying high voltage to the capacitance-gauge electrodes. These pushes may be given midway through the free-fall period, yielding corresponding changes in lateral velocity.
(iii) Each TMA is rotated around two horizontal axes by applying high voltage to the capacitance plates. These rotation maneuvers form the basis for determining Δz, the vertical CM-ORP separation of each TMA, with $\sigma(\Delta z) < 0.03\ \mu$m. Δz is important because it acts with the (measured) TMA rotation rate to produce an apparent TMA acceleration. While the CM-ORP separation also contributes to the uncorrected gravity-gradient acceleration, its effect cancels in the difference after a top–bottom swap. Similarly, the calibration maneuvers provide the basis for correcting the bias due to beam misalignment (cosine error) and to beam walk on imperfect optics.

In a perfect retroreflector cavity, translation of the input beam yields no change in S, the round trip optical path. Beam tilt would cause a cosine error. In our (real) system, the relative lateral motions and rotations of the TMA, vacuum chamber, and incoming beam, combined with angular errors in the retroreflectors and the wedged beamsplitter and compensator, yield errors that mimic an acceleration (Δg) of a few $10^{-11}\,\mathrm{m\,s^{-2}}$, which is comparable to the single-toss error from the laser gauge. To substantially remove these effects, we will produce and analyze the enriched data set resulting from the calibration maneuvers that exaggerate the 12 perturbations of the measurement system (per pair of TMA) described above. The perturbations will be observed to better-than-required accuracy using the capacitance gauges and a pair of "quad cells" that look at the incoming beam at the bottom and top of the chamber. The extra parameters associated with calibration maneuvers (e.g. Δz) will be estimated along with other experiment parameters.

Coriolis force can produce TMA acceleration far above the intended accuracy level. To address this systematic error, we will use a four-channel capacitance gauge

[a]The ORP is defined as the point around which a small rotation of the TMA does not cause a change in optical path. For a hollow retroreflector, the ORP is the geometric apex, and even a large rotation around the ORP causes no change in the optical path. For a solid retroreflector rotated around the ORP by θ, the lowest order correction to the optical path is proportional to θ^4.

for each TMA.[b] The POEM error budget requires that the transverse velocity be measured to 33 nm/s in each toss and that the bias in the average of these measurements be under 0.25 nm/s. In order to keep the stability requirement for the capacitance gauge at a reasonable level, we require that the TMA transverse velocity be under 10 μm/s. Since the TMA will pick up the chamber's transverse velocity at the time of launch, when the chamber will be moving upward at nearly 5 m/s, we require that the rail guiding the motion have angular deviations from vertical under $2 \cdot 10^{-6}$ rad. This, in turn, requires both a straight rail and careful leveling, which can be adjusted based on the TMA trajectories, as measured by the capacitance gauge.

2.1. *Tracking frequency laser gauge*

For POEM, we use the tracking frequency laser gauge (TFG) that we developed more than 15 years ago for POINTS,[1] an affordable space-based astrometric optical interferometer with a nominal single-measurement accuracy of 2 μas for a pair of bright stars separated by 90 ± 3 deg. Because of the close connection among size, weight, complexity, and cost, we kept the baseline length at 2 m and thus required high precision in the metrology in order to achieve the nominal single-measurement astrometric accuracy. The mission requirement was for a single metrology leg (laser gauge) to have an accuracy of 2 pm on time scales from 1 to 100 minutes. We could find no existing laser gauge that would meet that requirement. In particular, we looked at and rejected the standard precision laser gauge, the heterodyne interferometer.

As will become apparent, the TFG offers four advantages over the heterodyne gauge.[2] First, it is intrinsically free of the nm-scale cyclic bias that plagues the heterodyne gauges. It has only one beam and thus it cannot be subject to problems associated with separating beams of different frequencies. Second, it naturally operates not only in a nonresonant interferometer (Michelson, Mach–Zehnder, etc.), but also in a resonant cavity. Thus, additional accuracy is accessible when needed. However, operation in a nonresonant interferometer requires unequal paths. Third, the TFG can be used to measure absolute distance with little additional effort. Fourth, the TFG can suppress some additional errors associated with polarization sensitivity and, when used in a cavity, with beam alignment.

The TFG is an application of Pound–Drever–Hall locking, and Fig. 5 shows one realization. An optical signal from the variable frequency source (VFS) of an adjustable wavelength λ_{VFS} is phase modulated at a frequency f_m and introduced into the measurement interferometer, whose length, L, is to be determined. When λ_{VFS} is equal to λ_0, the wavelength at the intensity extremum with $N\lambda_0 = 2L$, the optical signal emerging from the interferometer is phase modulated but not

[b]The capacitance gauge is being developed in a collaboration with Winfield Hill of the Rowland Institute at Harvard.

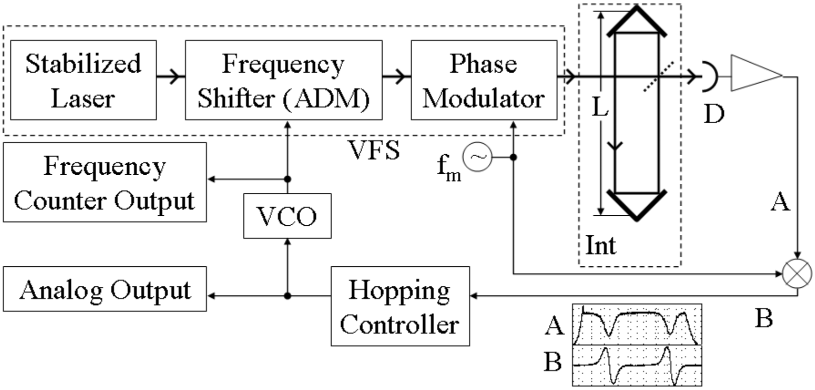

Fig. 5. TFG block diagram, classic realization.

amplitude modulated. When $\lambda_{\rm VFS}$ is away from λ_0, the optical signal emerging from the interferometer is both phase and amplitude modulated, resulting in an electrical signal at the detector output at f_m with a magnitude and sign that indicate the offset. Synchronous detection at f_m and filtering yield a signal that is used to control $\lambda_{\rm VFS}$, driving it back to λ_0. The corresponding optical frequency shift is measured by a frequency counter.

In any realization of the TFG, the usable range of the VFS will be limited either by the VFS or by the frequency counter. For most applications, the corresponding distance range would be too small. Therefore, we have introduced a nonlinear aspect into the TFG loop controller. It detects that it is running out of the frequency shifter's range and hops to a mode at the far end of the range, shifting the optical frequency by an integer multiple of the free spectral range, $\Phi = c/2L$. The hop is fast enough (about $1\,\mu$s) to be "unobserved" by the linear portion of the loop controller. We have demonstrated a rate of $5 \cdot 10^4$ hops/s, which corresponds to a linear velocity of 16 mm/s, using our HeNe version operating in a low finesse resonant interferometer for which $\Phi = 300\,$MHz.

If the precision of the TFG were limited by photon-counting statistics, then for $1\,\mu$W of HeNe (633 nm) power detected from a Michelson interferometer, the incremental distance uncertainty would be 0.06 pm after 1 s. The current TFG is limited by technical noise: $\sigma = 10\,$pm at either 1 or 10 samples per second.

The hopping provides an easy means of measuring absolute distance. By measuring the frequency shift before and after a hop, the TFG measures the free spectral range, Φ, of the measurement interferometer corresponding to the current length L. The estimate of L is then $Kc/2\delta F$, where δF is the frequency difference after hopping K fringes. The precision of the absolute distance measurement is

$$\sigma_T(L) = \frac{2}{\eta}\sqrt{\frac{\tau}{T}}\,\sigma_\tau(\delta L)\,, \tag{1}$$

where T and t are the integration times for absolute (L) and incremental (δL) distance, respectively. η is the fractional bandwidth, $\Delta F/F$, where F is the initial laser frequency.

One complication with this scheme comes from fluctuations in L due, for example, to vibration. There are two ways around this problem. Either use two lasers to read simultaneously or hop at a rate that reaches a portion of the disturbance spectrum where the noise is acceptably low. For sufficiently rapid hopping, vibration has this characteristic. For applications in air, path disturbances due to turbulence also diminish with frequency. The TFG does hop fast (50 kHz demonstrated) and the next generation TFG, which will be based on distributed feedback (DFB) lasers, will hop faster. Unlike most narrow-linewidth laser systems, the DFB laser provides rapid frequency shift for hopping without the use of an acousto-optic (AO) modulator. AO devices have a limited frequency-shift range, are bulky, prone to failure, require a free-space beam with attendant alignment issues, and have a time delay due to the acoustic propagation, which limits the achievable servo bandwidth and therefore the hop rate.

How large can η be? In the initial realization of the TFG, ΔF is limited to 500 MHz by the ADM. Since $\Phi = 300\,\mathrm{MHz}$ in the test rig and the HeNe operates at 633 nm, $\eta = 300\,\mathrm{MHz}/470\,\mathrm{THz} = 0.6 \cdot 10^{-6}$. We are developing the SL-TFG, a realization that uses DFB semiconductor lasers. In the SL-TFG, we could shift frequency both upward and downward from nominal to achieve $\Delta F = 2\,\mathrm{GHz}$, limited by our frequency counter and its internal dividers. (See Sec. 4.) For the DFB laser operating at 1550 nm, $\eta = 2\,\mathrm{GHz}/200\,\mathrm{THz} = 10^{-5}$.[c] A frequency counter with a greater range would permit an increase in η. For POEM, this must be a dual-channel counter with very small differential timing jitter.

2.2. *Capacitance gauge*

Coriolis force can produce TMA acceleration a_c far above the intended accuracy level: $a_c = 2\,v_{\mathrm{e-w}}|\omega|\cos(\mathrm{latitude})$ where $v_{\mathrm{e-w}}$ is the east–west component of the TMA velocity in the lab frame and the Earth rotation rate is $|\omega| = 7.292 \times 10^{-5}/\mathrm{s}$. To address this and other sources of systematic error, we will use a four-channel (later five-channel) capacitance gauge for each TMA. The POEM error budget requires that the transverse velocity be measured to 33 nm/s in each toss and that the bias in the average of these measurements be under 0.25 nm/s.

Figure 6 is a block diagram of the POEM capacitance gauge. It is of an unusual design because the TMA can neither be grounded nor connected directly to the sense amplifier. Instead, it is capacitively connected via an encircling cylindrical plate. Drive signals, applied through a tightly coupled transformer to plates that are segments of a cylinder, are at multiples of 2 kHz and in the range 10–18 kHz. These signals are kept small to limit their contribution to the vertical acceleration

[c]The SL-TFG is discussed briefly in the last section.

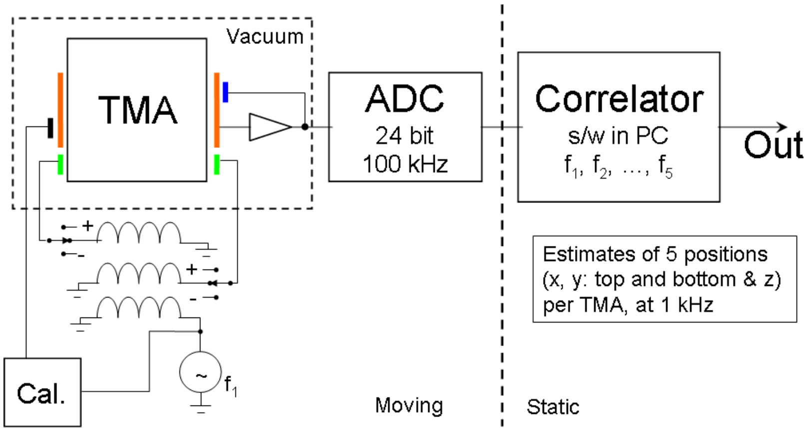

Fig. 6. Block diagram of the POEM capacitance gauge. The diagram shows the hardware associated with only one of the four drive signals.

of the TMA through fringing fields. With the nominal drive level of 0.1 V rms, we expect a position sensitivity better than 8 nm in 1 s in each channel. When the TMA is centered, the capacitive gaps are nominally 1 mm for both the drive and pickup plates. The optimized system has a single large pickup electrode and four pairs of small drive electrodes.

In the initial configuration, there are four pairs of drive plates covering two axes near both the top and the bottom of the TMA. The combination of displacement signals picked up by the encircling cylindrical plate is amplified and digitized before being sent to a PC for separate extraction in a software correlator. With the ADC trigger and the drive signals derived from the same stable oscillator, all 0.5 ms batches of data will have the same (integer) number of cycles of each of the drive signals, making possible a clean separation. The measurement intervals are a multiple of 0.5 ms.[d]

We use capacitive feedback around the sense amplifier to avoid phase shifts and a frequency-dependent response. Both the feedback capacitor and the calibration capacitor are machined into the assembly and must be mechanically stable. In order to keep the stability requirement for the capacitance gauge at a reasonable level,[e] we set the full scale at 10 μm and thus require that the TMA transverse velocity be under 10 μm/s. Since the TMA will pick up the chamber's transverse velocity at the time of launch, when the chamber will be moving upward at nearly 5 m/s,

[d]The motion system, discussed below, includes a high power (a few kW) PWM driver operating at 20 kHz. There is bound to be pickup in the CG from the lines to the motor. However, if the CG clock and the clock in the motor controller run accurately at their nominal speeds, then the 20 kHz signals from the motor controller will be well removed in the correlation process.
[e]The stability requirement is defined for this purpose as the ratio of the largest signal that can be processed to long-term change in that signal due to drift, e.g. from changing gain or bias. We take the stability requirement to be $4 \cdot 10^4$, based on engineering judgment.

we require that the rail guiding the motion have angular deviations from vertical under $2 \cdot 10^{-6}$. This, in turn, requires both a straight rail and careful leveling, which can be adjusted based on the capacitance gauge measurements.

3. Motion System

A key feature of POEM is that the experiment is conducted in a vacuum chamber that is placed in free fall with the TMA. In order to have a precision experiment based on a free fall time of 3/4 s, it is necessary to have a large number of repetitions, which suggests a need for rapid recycling. To meet this objective, we built a "bouncer" that catches the falling vacuum chamber and returns it to upward motion with little loss of energy or shock to the instrument inside the chamber. Once the chamber is again moving upward at the required speed (nearly 5 m/s), the TMA must be launched.

3.1. *Torsion bar bouncer*

It is our intention to run the laser gauge continuously, including during the bounce period when vertical acceleration reaches about 5 g. For this reason, to ease the job of the motor control servo, and to limit probe vibration so that the TMA are launched with minimal transverse velocity, it is essential that the bouncer produces minimal shock and vibration. This requirement rules out many obvious candidate designs. Having the chamber contact a cable (or flexible band) under tension results in a force on the chamber that initially grows linearly with cable deflection. We use a 1/4 inch steel cable, 62 cm long. It has a 0.1 kg mass but only 0.05 kg "effective mass" as seen by the falling chamber, which now has a mass of about 40 kg. (This will increase with Gen-II and Gen-III.) In addition, the cable probably flexes on initial contact, further reducing the shock to the moving system. Thus, as the chamber makes contact with the cable, there is a small bump as it loses one part in 800 of its velocity. The change of velocity is spread over a short interval of time by the flexing of the cable.

The next question is: How to store the energy of the falling chamber so that it can be returned to upward motion? Coil springs have internal modes that are problematic. Our initial design,[3] which used a ton of lead, a 5:1 lever, and a long cable running over pulleys, had two problems. First, on initial contact with the falling chamber, the cable experienced a longitudinal acceleration that excited an oscillation with the lead. Second, friction internal to the cable as it ran over the pulleys caused the system to fail to meet the efficiency requirement. The new bouncer uses torsion bars connected to the cable through stiff levers. Internal torsional modes of the bars are above 1 kHz and, to the extent excited, cannot contain much of the system's total energy since the bar's moment of inertia is very small compared to $M_{\text{chamber}} R_{\text{lever}}^2$. Tests show that bouncer energy loss is small and masked by uncertainty in the losses in the present slide. There is no sign of the torsion-bar bouncer introducing vibration, but the critical test awaits a quieter system based on an air-bearing slide.

3.2. *Air-bearing slide*

The present commercial slide uses instrument grade track rollers running on small (1/4 inch) but well-supported rails. At full speed, we find micron scale vibration, strongest in the 100–200 Hz band, yielding transverse velocity of 1 mm/s scale. We are in the process of implementing an air-bearing slide, as described in our original plans for this experiment.

We plan to use porous graphite bearings running on a granite beam. The undulations of the slope of the granite surface will need to under $2 \cdot 10^{-6}$ in the region where the cart is traveling when the TMA are launched. On linear scales shorter than the diameter of the air bearings (nominally 2 inch), the requirement can be relaxed because of the averaging that will take place. On large scales (say, over 1 m), the requirement can again be relaxed. Micron scale transverse displacement of the chamber, either after or well before TMA launch, has negligible effect on the intended results.

Such surface quality requirements are well within the capabilities of the large-optics industry. However, costs there are high, in part because the facilities are intended for making complex (aspherical) surfaces, not just the required flat. Fortunately, the requirements are just within the capability of the precision granite industry, which operates at significantly lower cost. As of this writing, we are preparing to place an order for a granite beam. Should we eventually wish to further reduce the transverse motion of the chamber due to the shape of the granite beam, we would consider connecting each air bearing to the moving assembly through an actuator (e.g. a PZT pusher) and using an inertial sensor to measure the required correction.

4. Key Technology Status and Conclusion

We have had a working TFG since the early 1990's. In the last few years, we have increased the frequency shift range, added the hopping capability, and demonstrated the measurement of absolute distance with the HeNe-based version. The HeNe TFG has operated successfully in the moving chamber, measuring the distance between the TMA. In this mode, it has tracked motion of several-μm amplitude and several-ms duration, consistent with brief episodes of TMA liftoff caused by the vibration, which was substantial at the time.

The standard frequency counter has dead time of up to 100 ms following each gate interval. We wish to be able to operate the TFG with samples as short as 0.1 ms although, for POEM, we anticipate 10 ms as a normal frequency measurement interval. Having dead time degrades the data set in three ways. First, only a portion of the available time is spent taking data; in some cases a small portion. Second, if there were no dead time, then certain errors made by the counter in sample n

would be made with the opposite sign in sample $n + 1$. Such "perfectly correlated noise" has a substantially smaller effect on estimates of the amplitudes of slowly varying quantities than does ordinary noise.[4] Third, a bias results from a mismatch of gate times for the two channels of the POEM counter for noncontiguous measurements.

A dual-channel frequency counter was built for POEM by Jim MacArthur, head of the Electronics Instrument Design Lab in Harvard University's Physics Department. This counter provides for contiguous measurements (no dead time) and precise synchronization between channels of the boundaries between measurement intervals. It operates to 200 MHz and contains $2\times, 4\times$, and $8\times$ dividers that permit a maximum count rate (each channel) of 400, 800, and 1200 MHz, respectively.

For the past few years, we have been working with DFB semiconductor lasers operating the 1550 nm communications band. Because of the large market for devices operating in this band, there are a wide variety of rugged, moderately priced components available. We have purchased a cavity with a finesse of 300, and locked a DFB laser to it. This cavity comprises a (45 mm OD $\times$ 150 mm) cylinder of Zerodur with an (13 mm) axial bore. Mirrors (one flat and one concave on its inner face) are optically contacted to the ends of the cylinder. They have identical v-coatings on their inner faces, providing 99.2% reflectivity. Further, they are wedged and have identical AR coatings on the outer faces to prevent these pieces of fused quartz from acting as spurious etalons.

We have locked two DFB lasers to adjacent orders of the cavity and measured the characteristics of the beat note. So far, we have only used a servo of rather low gain. We have since increased the servo gain substantially, and new results are pending.

The capacitance gauge is nearly completed. The architecture has long been established. We have received a preliminary version of the electrode assemblies and modified the probe to mount these around the TMA. All electronic components have been designed and are in various stages of fabrication, except for the preamp, for which only a basic design exists. We still need to decide how to package the electronics and connect through the probe vacuum flange. Most of the custom electronics will ride on or in the vacuum chamber.

The motion system is in the midst of an upgrade to reduce vibration. The new bouncer, based on a pair of torsion bars, has shown the high mechanical efficiency that we expected. Unlike the previous bouncer, it is left–right symmetric. Because of the higher efficiency of the new bouncer, the motor servo can be (and has been) tuned less aggressively. This results in a lower level of motor-driven vibration, yet the moving assembly still follows the intended trajectory within tens of μm.

We have measured the vibration in the present slide and found it too high. For this reason, we have begun to work on the long-intended upgrade to an air-bearing slide to replace the present commercial system that has wheels running along steel rails. According to the present plan, the air-bearing slide will use a granite beam and porous graphite bearings. Preliminary designs have been completed and no serious problem has been identified. Vendors have been found for all of the major components, and they are able to meet the requirements at a reasonable price. The hardware to make clean, dry compressed air has been delivered.

In summary, the SAO principle-of-equivalence measurement (POEM) is a Galilean test of the WEP divided into three developmental generations. The goal for the Gen-III version of the experiment is $\sigma(\Delta g)/g = 5 \cdot 10^{-14}$ for several pairs of substances. All Gen-I components are working and being tuned or modified for better performance. Work on some components originally described as part of Gen-II has started. These include the capacitance gauge, which is nearly finished, and the air slide, for which a preliminary design has been completed. The measurement system is being designed both for the control of systematic error and, where applicable, to be easily translated into a space-based version, for which we anticipate $\Delta g/g = 10^{-16}$.

Acknowledgments

We thank Kelzie Beebe (Harvard), Alexandru Ene (Harvard), Elizabeth Gould (Worcester Polytechnic), and Glen Nixon (Purdue), and high school student Alex McCaouley for skilful laboratory work. We thank colleagues Jim Faller (JILA), Robert Kimberk (SAO, Central Engineering), Tim Niebauer (Micro-g Corp.), and Doug Robertson (NGS/NOAA) for helpful discussions. We gratefully acknowledge support from the National Aeronautics and Space Administration through grant NNC04GB30G, and from the Smithsonian Institution directly and through the SAO IR&D program.

References

1. R. D. Reasenberg *et al.*, *Astron. J.* **32** (1998) 1731.
2. J. D. Phillips and R. D. Reasenberg, *Rev. Sci. Instr.* **76** (2005) 064501.
3. R. D. Reasenberg and J. D. Phillips, *Class. Quant. Grav.* **18** (2001) 2435.
4. R. D. Reasenberg, *Am. Inst. Aeronaut. Astronaut.* **10** (1972) 942.